Research Paper
J. Astron. Space Sci. 32(4), 357-366 (2015)
http://dx.doi.org/10.5140/JASS.2015.32.4.357

JASS Journal of Astronomy and Space Sciences

Minimum Number of Observation Points for LEO Satellite Orbit Estimation by OWL Network

Maru Park[1,2], Jung Hyun Jo[2,3†], Sungki Cho[2,3], Jin Choi[2,3], Chun-Hwey Kim[1], Jang-Hyun Park[2], Hong-Suh Yim[2], Young-Jun Choi[2], Hong-Kyu Moon[2], Young-Ho Bae[2], Sun-Youp Park[2], Ji-Hye Kim[2], Dong-Goo Roh[2], Hyun-Jung Jang[2], Young-Sik Park[2], Min-Ji Jeong[1,2]

[1]Department of Astronomy and Space Science, Chungbuk National University, Cheongju 28644, Korea
[2]Korea Astronomy and Space Science Institute, Daejeon 34055, Korea
[3]Korea University of Science and Technology, Daejeon 34113, Korea

By using the Optical Wide-field Patrol (OWL) network developed by the Korea Astronomy and Space Science Institute (KASI) we generated the right ascension and declination angle data from optical observation of Low Earth Orbit (LEO) satellites. We performed an analysis to verify the optimum number of observations needed per arc for successful estimation of orbit. The currently functioning OWL observatories are located in Daejeon (South Korea), Songino (Mongolia), and Oukaïmeden (Morocco). The Daejeon Observatory is functioning as a test bed. In this study, the observed targets were Gravity Probe B, COSMOS 1455, COSMOS 1726, COSMOS 2428, SEASAT 1, ATV-5, and CryoSat-2 (all in LEO). These satellites were observed from the test bed and the Songino Observatory of the OWL network during 21 nights in 2014 and 2015. After we estimated the orbit from systematically selected sets of observation points (20, 50, 100, and 150) for each pass, we compared the difference between the orbit estimates for each case, and the Two Line Element set (TLE) from the Joint Space Operation Center (JSpOC). Then, we determined the average of the difference and selected the optimal observation points by comparing the average values.

Keywords: OWL-Net, LEO, TLE, optical observation, orbit estimation

1. INTRODUCTION

Currently, a number of Korean space assets are located in Low Earth Orbit (LEO) and Geo-Stationary Orbit (GEO). In Near Earth space, there are a large number of artificial space objects concentrated in LEO and GEO. This concentration is especially severe in LEO, to such levels that conjunction events occur frequently, including the collision between Iridium 33 and COSMOS 2251 in 2009. Accordingly, the Korea Astronomy and Space Science Institute (KASI) is developing an Optical Wide-field Patrol Network (OWL-Net) to monitor Korean space assets (Park et al. 2012). To anticipate and respond to space-object conjunctions effectively, the location and speed of proximal space objects must be known.

Telescopes and observation time in Korea that could be utilized for space-object monitoring are limited. To use such limited resources effectively, it is important to find the minimum number of observation points that would allow estimation of orbits with an appropriate degree of precision. Choi et al. (2015) observed GEO satellites and estimated their orbits to determine the optimum number of observations. The numbers of observation points used for orbit estimation were 30, 60, 100, 150, 200, 300, 400, and 600. From these, the degrees of precision of the estimated orbits were compared. Moreover, the estimated orbits and Two Line Element set (TLE) were compared and it was found that the estimated orbit became closer to TLE when there

Received Oct 30, 2015 **Revised** Nov 20, 2015 **Accepted** Nov 24, 2015
†**Corresponding Author**
E-mail: jhjo39@kasi.re.kr, ORCID: 0000-0003-1906-8075
Tel: +82-42-865-3238, Fax: +82-42-865-3358

were more observation points. In this study, the number of observation points for each pass (of LEO satellites) were 20, 50, 100, and 150 for orbit estimation, and estimation based on all the observation points (320). Comparison of the estimated orbits and the TLE were conducted afterwards. In this paper, a pass is defined as one passage of a satellite across the sky over the observatory. A shot refers to one image; one observation point is that obtained from the center point of a satellite streak.

Types of space-object monitoring systems include radar, laser, and optical observation methods. Lee et al. (2004) explained that the optical observation method has some advantages in identifying a situation in space, including in GEO. For this optical observation method, the monitoring of space objects is possible when the light reflected from space objects is brighter than the space background. Therefore, when sufficiently bright light reaches the observatory, recognizing the space condition is possible regardless of the distance. The optical observation method is advantageous in obtaining angular data including Right Ascension and Declination; however, it is not possible to obtain distance information directly, this way. Gauss and Laplace developed a method of determining distance and initial orbit of natural celestial bodies approximately 200 years ago.

Because we used an orbit estimation technique of an over-determined system, the initial orbit was not determined using the methods of Gauss or Laplace. Instead, TLE (provided by Space Track) was used as the initial orbit. For the orbit estimation of a satellite, the Orbit Determination Tool Kit (ODTK) program (developed by Analytical Graphics, Inc.: AGI), was utilized. In addition, the estimated orbit and TLE were compared using the System Tool Kit (STK) developed by AGI. Among the publicly available satellite orbits, TLE data provides the orbital data for most satellites. Regarding the accuracy of TLE, Vallado et al. (2013) showed that TLE, propagated with Simplified General Perturbations 4 (SGP4), maintained a degree of accuracy within 10 km of the actual orbits. Thus, with a Root Mean Squared (RMS) average distance of 10 km between the estimated orbit and the TLE, this method is considered appropriate for orbit estimation.

In this paper, orbit estimation was performed according to several groups of observation points of increasing number for each LEO satellite pass, and these were compared with results obtained using TLE. Seven LEO satellites were observed including Gravity Probe B, Seasat 1, ATV-5, CryoSat-2, COSMOS 1455, COSMOS 1726, and COSMOS 2428. The orbit estimation results were compared with TLE to obtain the distance difference according to time. Moreover, the difference variation between the TLE and the orbit estimation results was analyzed according to the number of estimation points.

2. OPTICAL WIDE FIELD PATROL NETWORK (OWL-NET)

Currently operating observatories of OWL-Net are located in Daejeon (South Korea), Songino (Mongolia), and Oukaïmeden (Morocco), while observatories in Israel and the U.S. are under construction. The Daejeon Observatory is a test-bed that inspects each system and performs operation testing. Fig. 1 and Table 1 show the geographic locations and coordinates of each observatory.

Fig. 2 shows the OWL-Net dome, which is a fully open system. Table 2 shows that the optical telescope diameter is 50 cm, with a Field of View (FOV) of 1.10 degree of arc, and an Alt-Azi type mount. Fig. 3 shows the chopper installed in front of the CCD camera to obtain numerous observation points with a single exposure. When the CCD camera receives an exposure command, the chopper initiates rotation and the CCD camera opens and closes by means of the chopper blade. When the CCD camera is open, satellite streaks are obtained. The series of streaklets for satellites appear as dotted lines in the obtained images.

Fig. 1. Locations of the operating OWL-Net observatories: Songino, Mongolia; Oukaïmeden, Morocco; and Daejeon, Korea (test-bed).

Table 1. Locations of OWL-Net Observatories

#	Country	City	Latitude	Longitude	height(km)
Test bed	Korea	Daejeon	36:23:51.4851 N	127:22:32.4453 E	0.139
OWL 1	Mongol	Songino	47:53:10.0538 N	106:20:05.1414 E	1.674
OWL 2	Morocco	Oukaïmeden	31:12:23.3000 N	-07:51:59.4000 E	2.725

Fig. 2. The optical tube assembly on an Alt-Azi mount at the test-bed of OWL-Net.

Table 2. Specifications of the OWL-Net optical telescope

Item	Value
Diameter	50 cm
Effective focal length	1,493.46 mm
F/number	2.99
FOV	1.10 deg
Mount	Alt-Azi

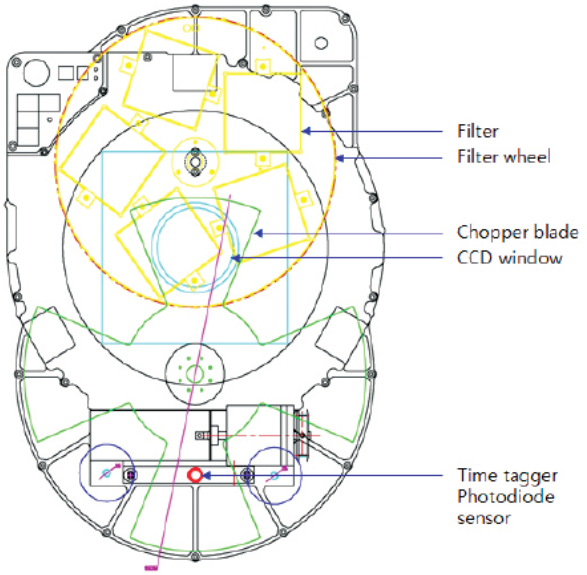

Fig. 3. Design of the wheel station housing of a CCD camera, a chopper system, and a filter wheel of OWL-Net (Park et al. 2013).

The OWL-Net can use different observation modes when monitoring LEO and GEO satellites. For the LEO satellite observation mode, the chopper is used because stars are tracked using a sidereal clock drive (derotator). Therefore, stars are detected as points and satellites are detected as streaks. For the GEO satellite observation mode, neither the chopper nor the tracking function may be used. Normally, the OWL-Net satellite observation-mode detects stars as points and satellites as streaks. The observation strategy for GEO satellite was studied by Choi et al. (2011, 2015). In this study, to establish an effective observation strategy for LEO satellites, an LEO satellite observation mode was employed.

The observation images were processed using a preprocessing program developed by Park et al. (2013). This preprocessing program detects satellite streaks in the images to determine the satellite streak epoch time, right ascension, and declination. Currently, this preprocessing program is subject to detection errors, such as occasionally failing to detect satellites or misidentifying stars as satellites. With this program, the time and coordinates are obtained using different methods. The time information is obtained through the time history of the CCD camera's observation window opening and closing due to the action of the chopper, while the right ascension and declination are obtained using the acquired streak coordinates and absolute coordinates of the background stars. According to Son et al. (2015), the time information of the OWL-Net can be synchronized to the order of 0.001 s using the Network Time Protocol (NTP). The obtained time and coordinates are sequentially recorded. For example, as can be seen in Fig. 4, the small circle is the detected satellite's coordinates, as obtained using the preprocessing program, the white boxes are the sequentially recorded time data, and the black boxes are the sequentially recorded coordinate data. Black No. 3 is a misidentification of a star near a streak as a satellite. In the recordings, the satellites are recorded as being at the coordinates of Black No. 3 for the time of White No. 3, and at the coordinates of Black No. 4 for the time of White No. 4. As a result, the time and coordinate data become mismatched, causing error in the orbit determination using this observation data. This problem is similar to that described by Jo et al. (2015). Such detection error causes mismatches between the time and coordinate data. Therefore, the recorded time information and the corresponding satellite streak must be accurately re-matched to compensate for the detection error.

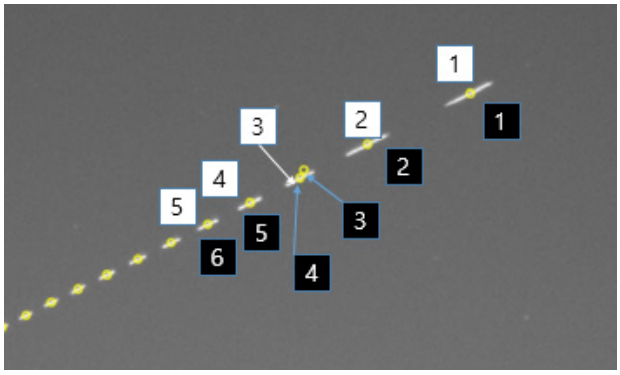

Fig. 4. Partial shot of Gravity Probe B observed 2 October 2014 at the test-bed.

3. POST CORRECTION OF OPTICAL OBSERVATION DATA BY OWL-NET

In this study, LEO satellites ATV-5, Gravity Probe B, CryoSat-2, Seasat 1, COSMOS 1455, COSMOS 1726, and COSMOS 2428 were observed. The observation subjects were LEO satellites observed for over three days by OWL-Net. Of note, ATV-5 was observed through international cooperation with the Defense Advanced Research Projects Agency (DARPA) and performed re-entry on 15 February 2015. Table 3 shows the North American Aerospace Defense Command Catalogue Number (NORAD ID), perigee altitude, apogee altitude, and eccentricity of the satellites from Space Track.

In this study, data from the Songino OWL-Net observatory and the Daejeon OWL-Net test-bed were used. The data, after compensation for detection error, are shown in Tables 4 and 5. Only passes with more than 145 observation points were used. For ATV-5, two passes obtained on 15 February 2015, were used.

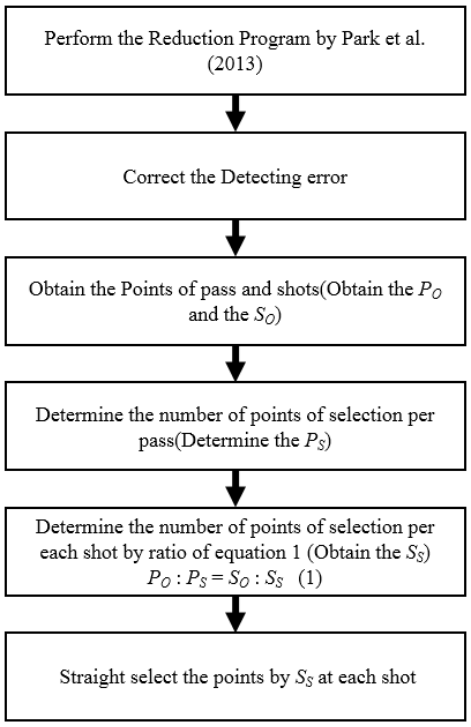

Fig. 5. Selection process of points in each shot.

4. METHODS OF ORBIT DETERMINATION AND RESULTS

In this study, we focused on determining the minimum number of effective observations per pass, needed to maximize the efficiency of the OWL-Net observation strategy. Several sets of observation points of increasing number (20, 50, 100, and 150), as well as all points together (320), were used for each pass in the orbit-estimation experiment. For this experiment, both detected streaks and non-detected streaks were considered to reflect the effect of detection error when selecting observation points. When the satellite passed over the sky above the observatory, one observation pass was completed and this pass was observed (recorded) in numerous shots. The number of observation points obtained from a pass (P_O) and the number of observation points obtained from a shot (S_O) were determined. Fig. 5 shows the process of determining the observation points from each shot. In the figure, P_S is the number of observation points that could be selected from a pass and S_S is the number of observation points that could

Table 3. Orbital characteristics of the observed satellites

Observation Target		Orbit(km)		
Satellite	NORAD ID	Perigee	Apogee	Eccentricity
ATV 5	40103	368	405	0.0013728
COSMOS 1455	14032	516	543	0.0019497
COSMOS 1726	16495	507	526	0.0013828
COSMOS 2428	31792	845	857	0.0007984
CryoSat-2	36508	712	726	0.0009476
Gravity Probe B	28230	635	638	0.0002320
SEASAT 1	10967	747	749	0.0001213

Table 4. Orbital characteristics of the observed satellites

Satellite	Date	Points per pass	Points per shot																			
			1	2	3	4	5	6	7	8	9	10	11	12	13	14	15	16	17	18	19	20	21
CryoSat-2	20150524	453	69	76	50	62	94	102															
	20150525	1,595	56		43		71	122	119	109	108	103	100	94	91	85	80	74	73	70	70	71	56
	20150528	256								69	86	101											
	20150603	706										99	92	87	81	77	73	70	66		61		
Gravity Probe B	20141104	279					52	56		78	93												
	20141105	575		89	81	67	54	46				65	79	94									
	20141106	94									94												
Seasat 1	20141117	223	67	50	20					21		65											
	20141119	209				82	69	58															
	20141120	104							104														

Table 5. Statistics of satellite observation at the OWL-Net Songino Observatory

Satellite	Date	Points per pass	Points per shot																				
			1	2	3	4	5	6	7	8	9	10	11	12	13	14	15	16	17	18	19	20	21
ATV-5	20150215	506		52	52	81	70	61	50	45			43	52									
	20150215	155			48	51		56															
COSMOS 1455	20141101	375	93	76	51	26			13	45	71												
	20141104	341		74	61	42	29	32	45	58													
	20141106	86									86												
COSMOS 1726	20141101	272		68	38	15					62	89											
	20141102	145		53	17			21		54													
	20141103	354	87	80		21	15		30	48	73												
	20141105	250							39	55	70	86											
	20141106	84										84											
COSMOS 1455	20150210	825					99	90	84	82	83	89	99	102	97								
	20150211	178											45	121	12								
	20150212	994		110	129	118	109	101	96		99	111	121										
	20150213	1,133		142	130	119	109	103	99	98	100	112	121										
	20141105	250							39	55	70	86											
	20141106	84										84											
Gravity Probe B	20141101	819	113	97	82	68	54	41	33	44	61	78	95	53									
	20141102	731	113	99	55	68	68	70	77	85	96												
	20141103	287		83	95	109																	
	20141104	442				43	54	45	43	51	62	77	67										
	20141105	366	112	91	87	76																	
	20141106	553	115	90		81	80	85		102													
Seasat 1	20141121	380								51	59	72		99	99								
	20141123	130							50				80										
	20141127	252										74	85	93									

be selected from a shot.

Orbit estimation was performed using the ODTK developed by AGI. Table 6 shows the input values, which were changed for the ODTK setup. When the position and speed uncertainty were reduced, the problem of non-convergence occurred for ODTK, so the values for position and speed uncertainty were set to be relatively large.

To establish a precise dynamics model, all acceleration terms supported by ODTK were set as shown in Table 7. Two largest values among the satellite height, width, and depth were multiplied, and set as the satellite surface area.

Compensation of the observation data was performed with regard to diurnal and annual aberrations, detection error, and Light Travel Time. The detection error and Light Travel Time compensations were applied when the ODTK input file was created, while the compensation for diurnal and annual aberrations was directly applied within ODTK.

The steps for using ODTK were, in the order used for initial orbit determination, least square method, filter, and smoother. In this study, we found frequent occurrence of the least square method tracking the wrong local minimum. Thus, instead of using the least square method results as the initial value for the filter, TLE was used as the initial value for the filter. The TLE used here was obtained from Space Track.

Finally, using the STK developed by AGI, the filter result

Table 6. List of ODTK configurations

Object	Properties	Value
Satellite	Initial orbit state	TLE of Space Track
	Mass	Obtained from reference
	Area	Obtained from reference
	Cd	2.2
	R	1,000 m
	I	2,000 m
	C	100 m
	dot R	1 m/s
	dot I	1 m/s
	dot C	1 m/s
Observatory	Measurement Statistics Elements	RA, Dec
	Sigma	20 arcsec
	Half Life	1 min
	White Noise Sigma	3 arcsec
	Estimation bias	TRUE
	Antenna Type	Optical
	Aberration	all
Filter	Start Time	First observation time
	Nominal Sigma	100

from the ODTK was compared with the TLE propagation result. The TLE provided by JSpOC and the orbit estimation results were compared to determine the precision of the orbit estimation. With TLE as the reference, the distance differences for the radial, in-track, and cross-track coordinates of the estimated orbit were set as the precision indicators. In addition, the RMS average was obtained for the distance difference. Figs. 6–19 and Table 8 show the

Table 7. List of acceleration terms applied in ODTK to estimate orbits

Perturbation	Acceleration term
Gravity force	EGM 96, 70 X 70 Gravity force of Sun, Moon and other Planets Tide force by ground and ocean General relative effect
Drag	CIRA 1972 Model Ballistic Coefficient(BC)=Cd*A/m[1)]
Solar radiation pressure	Spherical Radiation Model Shadow of Earth and Moon

[1)]The dimension and mass of each satellite were obtained from eoPortal Directory (2015a, b), ESA (2015), Kosmonavtika (2015), and Everitt & Parkinson (2006).

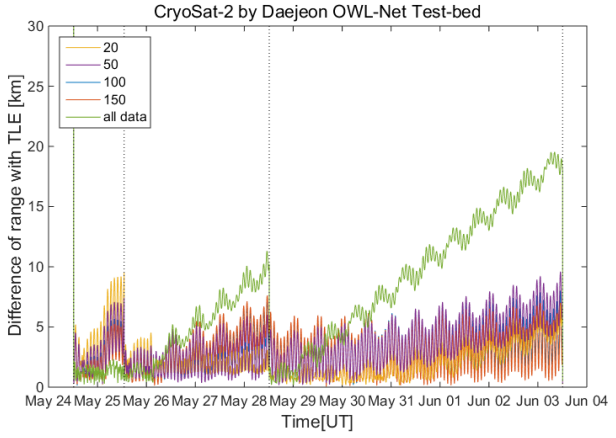

Fig. 6. Differences of the range in Radial-In track-Cross track coordinates between the estimated orbits of CryoSat-2 observed on 24 May–03 June 2015 at the Daejeon OWL-Net Test-bed, with sets of differing number of observations, and TLE with 11 epochs as a reference orbit (The vertical solid lines represent an observation epoch, and the result of each set is distinguished with colors, as shown in the box at the upper left corner of the figure).

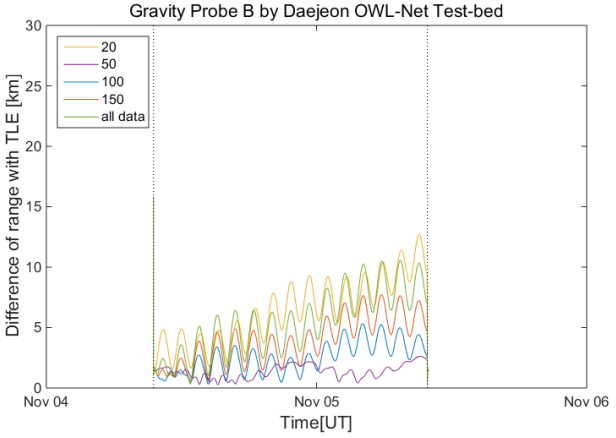

Fig. 7. Differences of the range in Radial-In track-Cross track coordinates between the estimated orbits of Gravity Probe B observed on 04–05 November 2014 at the Daejeon OWL-Net Test-bed, with sets of differing number of observations, and TLE with five epochs as a reference orbit (The vertical solid lines represent observation epochs, and the result of each set is distinguished with colors, as shown in the box at the upper left corner of the figure).

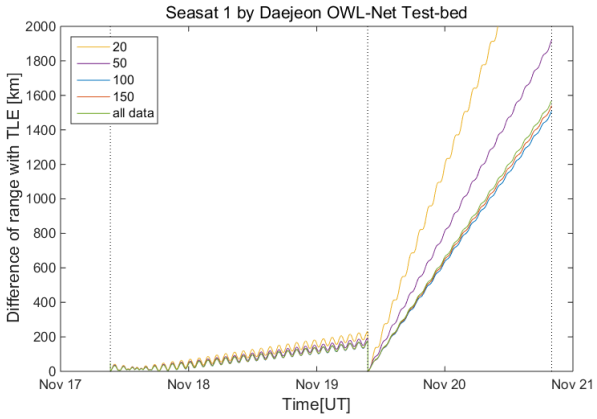

Fig. 8. Differences of the range in Radial-In track-Cross track coordinates between the estimated orbits of Seasat 1 observed on 17–20 November 2014, at the Daejeon OWL-Net Test-bed, with sets of differing number of observations, and TLE with five epochs as a reference orbit (The vertical solid lines represent observation epochs, and the result of each set is distinguished with colors as shown in box at the upper left corner of the figure).

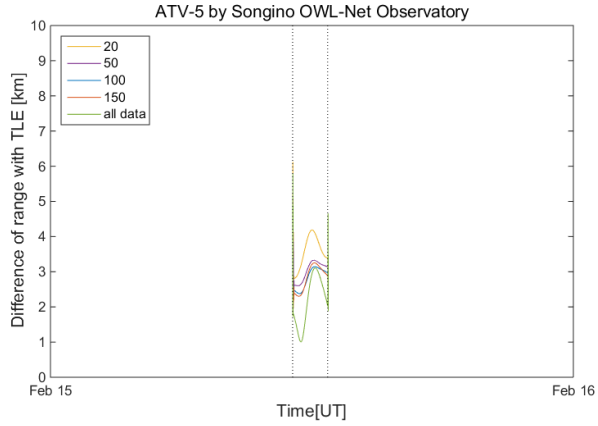

Fig. 9. Differences of the range in Radial-In track-Cross track coordinates between the estimated orbits of ATV-5 observed on 15 February 2015 at the Songino OWL-Net Observatory, with sets of differing number of observations, and TLE with three epochs as a reference orbit (The vertical solid lines represent observation epochs, and the result of each set is distinguished with colors, as shown in the box at the upper left corner of the figure).

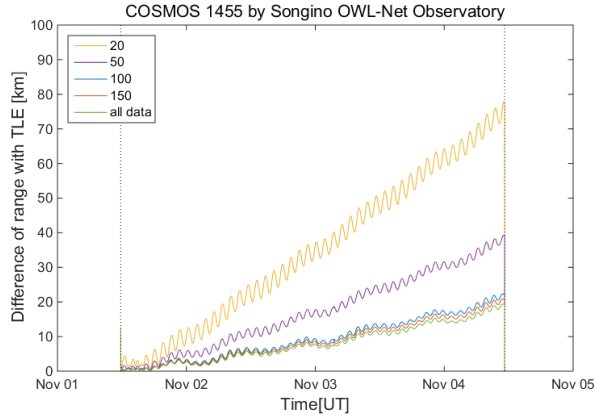

Fig. 10. Differences of the range in Radial-In track-Cross track coordinates between the estimated orbits of COSMOS 1455 observed on 01–04 November 2014 at the Songino OWL-Net Observatory, with sets of differing number of observations, and TLE with six epochs as a reference orbit (The vertical solid lines represent observation epochs, and the result of each set is distinguished with colors as shown in the box at the upper left corner of the figure).

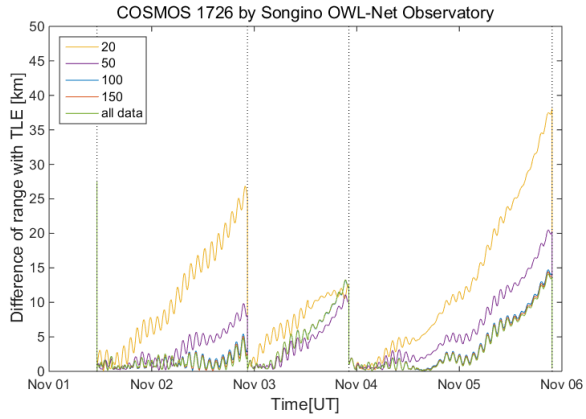

Fig. 11. Differences of the range in Radial-In track-Cross track coordinates between the estimated orbits of COSMOS 1726 observed on 01–05 November 2015 at the Songino OWL-Net Observatory, with sets of differing number of observations, and TLE with six epochs as a reference orbit (The vertical solid lines represent observation epochs, and the result of each set is distinguished with colors as shown in the box at the upper left corner of the figure).

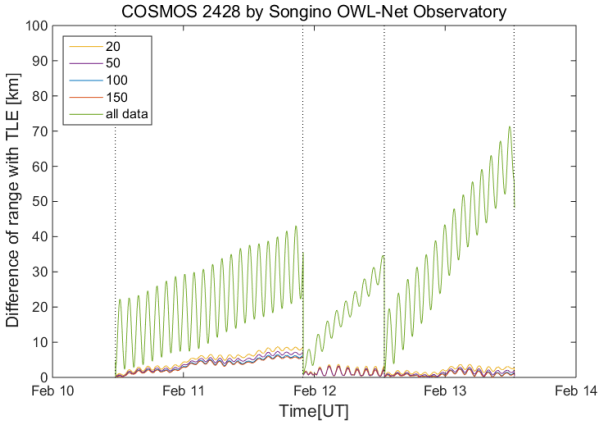

Fig. 12. Differences of the range in Radial-In track-Cross track coordinates between the estimated orbits of COSMOS 2428 observed on 10–13 February 2015 at the Songino OWL-Net Observatory, with sets of different number of observations, and TLE with thirteen epochs as a reference orbit (The vertical solid lines represent observation epochs, and the result of each set is distinguished with colors as shown in the box at the upper left corner of the figure).

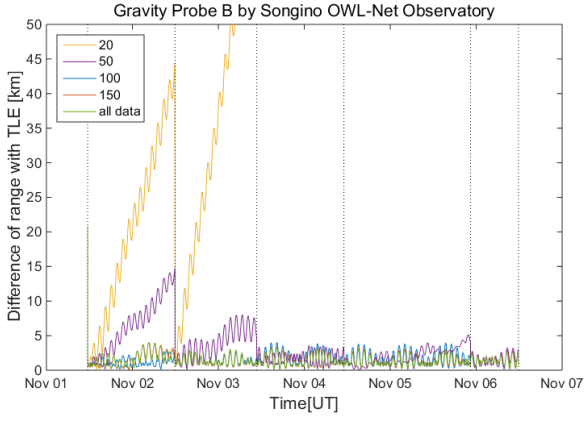

Fig. 13. Differences of the range in Radial-In track-Cross track coordinates between the estimated orbits of Gravity Probe B observed on 01–06 November 2015 at the Songino OWL-Net Observatory, with sets of different number of observations, and TLE with seven epochs as a reference orbit (The vertical solid lines represent observation epochs, and the result of each set is distinguished with colors as shown in the box at the upper left corner of the figure).

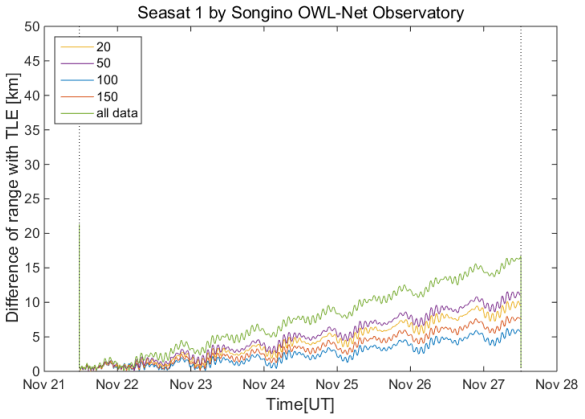

Fig. 14. Differences of the range in Radial-In track-Cross track coordinates between the estimated orbits of Seasat 1 observed on 21–27 November 2014 at the Songino OWL-Net Observatory, with sets of differing number of observations, and TLE with seven epochs as a reference orbit (The vertical solid lines represent observation epochs, and the result of each set is distinguished with colors as shown in the box at the upper left corner of the figure).

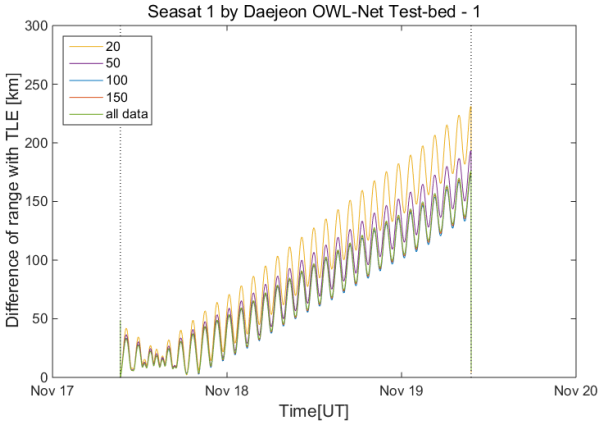

Fig. 15. Differences of the range in Radial-In track-Cross track coordinates between the estimated orbits of Seasat 1 observed on 17–19 November 2014 at the Daejeon OWL-Net test-bed with sets of differing number of observations, and TLE with three epochs as a reference orbit (The vertical solid lines represent observation epochs, and the result of each set is distinguished with colors as shown in the box at the upper left corner of the figure).

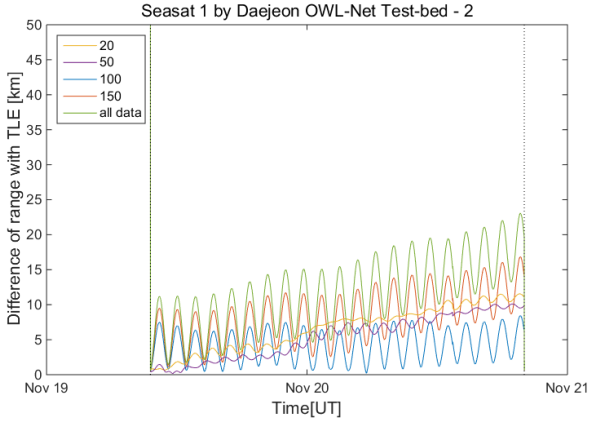

Fig. 16. Differences of the range in Radial-In track-Cross track coordinates between the estimated orbits of Seasat 1 observed on 19–20 November 2014 at the Daejeon OWL-Net test-bed with sets of differing number of observations, and TLE with three epochs as a reference orbit (The vertical solid lines represent observation epochs, and the result of each set is distinguished with colors as shown in the box at the upper left corner of the figure).

Table 8. Difference between TLE and RMS mean range of estimated orbit

Observatory	Satellite	Difference between TLE and RMS mean range of estimated orbit (km)				
		20	50	100	150	all
Testbed	CRYOSAT_2	3.25	3.64	2.82	2.61	8.10
	Gravity_Probe_B	6.15	1.39	2.46	3.62	4.26
	Seasat_1	646.13	451.71	362.65	372.12	400.97
Songino	ATV-5	3.49	2.99	2.79	2.70	2.48
	Gravity_Probe_B	390.66	3.12	1.46	1.42	1.53
	COSMOS_1455	34.75	16.87	9.03	8.25	7.13
	COSMOS_1726	10.93	4.72	3.21	3.12	3.02
	COSMOS_2428	3.34	2.63	2.17	1.99	23.40
	Seasat_1	4.33	5.02	2.44	3.29	7.17

obtained results. In Figs. 6–19, the black vertical line refers to the time of observation. Fig. 15 shows the result that was obtained using the optical observation data of Seasat 1 on 17 and 19 November 2014, by the Daejeon OWL-Net test-bed. Fig. 16 shows the results obtained using optical observation data of the same subject and by the same observatory but for different dates (19 and 20 November 2014). Figs. 17–19 show results obtained using only the optical observation data of the Daejeon OWL-Net test-bed for Seasat 1 on 17, 19, and 20 November 2014.

5. SUMMARY

Comparing the orbit estimation results according to the observation point numbers for 7 LEO satellites revealed that the use of more observation points led to more accurate estimations of orbits, except for Seasat 1 and Gravity Probe B, as shown in Figs. 6–14. When comparing the orbit estimation results for Seasat 1 and Gravity Probe B with those of the other satellites, it was difficult to explain the abnormality of the orbit estimation results with anything other than errors in the observation data or errors in the orbit estimation filter (shown in Figs. 7–8 and Figs. 13–14). In addition, comparison between the orbit estimation conditions of the other satellites, except for the two satellites in question, shows that the possibility of an error in the orbit estimation filter is very low. Thus, the source of the errors was thought to be in the observation data obtained from the optical observations of Seasat 1 and Gravity Probe B.

Though the Gravity Probe B and Seasat 1 had similar observation periods, the estimated orbits obtained from each observatory were clearly different. It is thought that there is a measurement time bias in one of the two observatories, or in both observatories. The presence of significant error in many observation points is recognized by ODTK due to the measurement time bias, resulting in

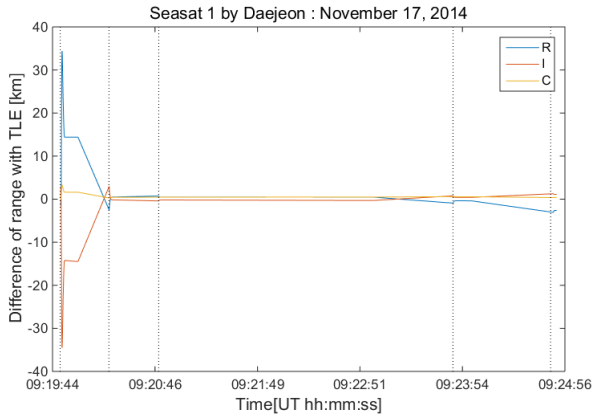

Fig. 17. Differences of the range in Radial-In track-Cross track coordinates between the estimated orbits of Seasat 1 observed on 17 November 2014 at the Daejeon OWL-Net test-bed, with sets of different number of observations, and TLE with two epochs as a reference orbit (The vertical solid lines represent observation epochs, and the result of each set is distinguished with colors as shown in the box at the upper left corner of the figure).

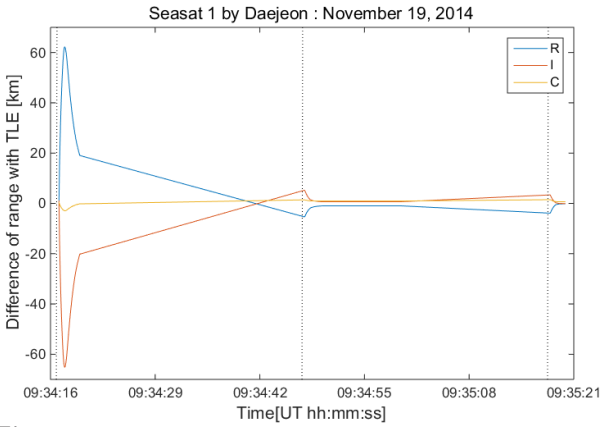

Fig. 18. Differences of the range in Radial-In track-Cross track coordinates between the estimated orbits of Seasat 1 observed on 19 November 2014 at the Daejeon OWL-Net test-bed, with sets of differing number of observations, and TLE with two epochs as a reference orbit (The vertical solid lines represent observation epochs, and the result of each set is distinguished with colors as shown in the box at the upper left corner of the figure).

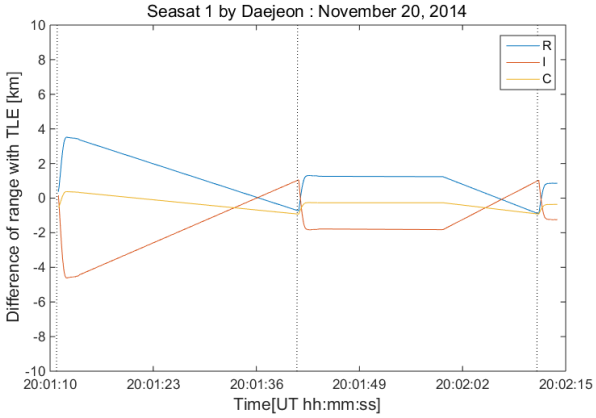

Fig. 19. Differences of the range in Radial-In track-Cross track coordinates between the estimated orbits of Seasat 1 observed 20 November 2014 at the Daejeon OWL-Net test-bed, with sets of differing number of observations, and TLE with two epochs as a reference orbit (The vertical solid lines represent observation epochs, and the result of each set is distinguished with colors as shown in the box at the upper left corner of the figure).

the rejection of these points, and their not being used in the orbit estimation. When Seasat 1 observation data for three days was processed as 1 degree of arc, the result shown in Fig. 8 was obtained; however, when the same observation data were processed in relation to a daily base, the orbit estimation results shown in Figs. 17–19 were obtained. This shows that when the observation data for Seasat 1 is used on a daily base, there is no significant deviation from TLE. In Fig. 15, it can be observed that the estimated orbit of Seasat 1 deviated greatly from TLE. However, when data for a specific day is processed, as shown in Fig. 16, the orbit accuracy is fairly well maintained. In this case, there is no close correlation between the number of observation points used for the data processing, and the improvement in accuracy. From the above results, it was determined that an adequate orbit was obtainable through orbit estimation using individual arcs; however, due to the presence of very different levels of measurement time-bias between the Seasat 1 observation data on 17 and 19 November 2014 at the Daejeon OWL-Net test-bed, orbit estimation failed when it was attempted using observation data as one long arc.

In Table 8, it can be seen that regardless of the number of observation points for CryoSat-2, ATV-5, and COSMOS 2428, the RMS average difference in distance from TLE was within 10 km. In the cases of COSMOS 1455 and COSMOS 1726, the RMS average difference in distance from TLE was within 10 km when the numbers of observation points were 100 and 50, respectively. Thus, when the number of observation points is greater than 100, the RMS average distance difference between the estimated orbit and TLE is within 10 km. For COSMOS 2428, the distance difference with TLE is greater when using all the observation points, than when using 150 points. This is thought to be due to not selecting an observation point that significantly includes observation errors.

The observation periods for Gravity Probe B and Seasat 1 at the test-bed and Songino Observatories were either similar or overlapped. The Gravity Probe B observed from the test-bed, and Seasat 1 observed from the Songino Observatory showed tendencies of varying orbit estimation accuracy, regardless of the number of observation points. Therefore, Gravity Probe B and Seasat 1 used the observations of both observatories, and orbit estimations were not performed.

In conclusion, the distance between the estimated orbit and TLE for LEO satellites was within 10 km when the number of observation points for each pass was greater than 100, in most cases. When the number of observation points per pass increased, the estimated orbit and TLE converged. Unlike for generally known orbit estimation theory, using all the observation points for orbit estimation resulted, in some cases, in the reduction of the accuracy of orbit estimation. Moreover, the exceptionally unacceptable orbit estimation results obtained when using observation data from a specific observatory on a specific date are thought to be due to the presence of measurement-time bias for each observatory that cannot be estimated, and that has temporal variation in its magnitude. Therefore, until the problem of measurement-time bias for each observatory can be clearly addressed and resolved, using all observation points for orbit estimation will not necessarily lead to improved results.

ACKNOWLEDGMENTS

This study was partially supported by the National Research Council of Fundamental Science & Technology through a National Agenda project "Development of Electro-optic Space Surveillance System" and matching funds from the Korea Astronomy and Space Science Institute.

REFERENCES

Choi J, Jo JH, Choi YJ, Cho GI, Kim JH, et al., A Study on the Strategies of the Positioning of a Satellite on Observed Images by the Astronomical Telescope and the Observation and Initial Orbit Determination of Unidentified Space Objects, J. Astron. Space Sci. 28, 333-344 (2011). http://dx.doi.org/10.5140/JASS.2011.28.4.333

Choi J, Jo JH, Roh KM, Son JY, Kim MJ, et al., Analysis of the angle-only orbit determination for optical tracking strategy of Korea Geo satellite, COMS, Adv. Space Res. 56, 1056-1066 (2015). http://dx.doi.org/10.1016/j.asr.2015.06.005

eoPortal Directory, CryoSat [Internet], cited 2015a, available from: https://directory.eoportal.org/web/eoportal/satellite-missions/c-missions/cryosat#footback10)

eoPortal Directory, Seasat [Internet], cited 2015b, available from: https://directory.eoportal.org/web/eoportal/satellite-missions/s/seasat#foot9%29

ESA, ATV configuration [Internet], cited 2015 Jul 10, available from: http://www.esa.int/Our_Activities/Human_Spaceflight/ATV/ATV_configuration

Everitt F, Parkinson B, The Gravity Probe B EXPERIMENT, Post Flight Analysis - Final Report (2006).

Jo JH, Choi J, Park M, Son JY, Bae Y, et al., Early CAL/VAL process for an optical tracking system by Korea, Proceedings of the 16th AMOS Conference, Hawaii, United States, 15-18 Sep 2015.

Kosmonavtika, Tselina [Internet], cited 2015 Jan 19, available from: http://www.kosmonavtika.com/satellites/tselina/tech/tech.html

Lee WK, Lim HC, Park PH, Youn JH, Yim HS, et al., Orbit Determination of GPS and KOREASAT 2 satellite using Angle-Only Data and Requirements for Optical Tracking System, J. Astron. Space Sci. 21, 221-232 (2004). http://dx.doi.org/10.5140/JASS.2004.21.3.221

Park JH, Choi YJ, Jo JH, Moon HK, Yim HS, et al., Korean Space Situational Awareness Program: OWL Network, Proceedings of the 13th AMOS Conference, Hawaii, United States, 11-14 Sep 2012.

Park SY, Keum KH, Lee SW, Jin H, Park YS, et al., Development of a Data Reduction Algorithm for Optical Wide Field Patrol, J. Astron. Space Sci. 30, 193-206 (2013). http://dx.doi.org/10.5140/JASS.2013.30.3.193

Son JY, Jo JH, Choi J, Kim BY, Yoon JN, et al., Optical Orbit Determination of a Geosynchronous Earth Orbit Satellite Effected by Baseline Distances between Various Ground-based Tracking Stations Ⅱ: COMS Case with Analysis of Actual Observation Data, J. Astron. Space Sci. 32, 229-235 (2015). http://dx.doi.org/10.5140/JASS.2015.32.3.229

Vallado DA, Agapov V, Orbit Determination Results From Optical Measurements, Proceedings of the European Space Astronomy Centre, Madrid, Spain, 3-6 May 2010.

Vallado DA, Hujsak RS, Johnson TM, Seago JH, Woodburn JW, Orbit Determination Using ODTK Version 6, Proceedings of the European Space Astronomy Centre, Madrid, Spain, 3-6 May 2010.

Vallado DA, Virgili BB, Flohrer T, Improved SSA Through Orbit Determination of Two-Line Elements Sets, Proceedings of the 6th European Conference on Space Debris, Darmstadt, Germany, 22-25 Apr 2013.